Journal of Plasma Physics
http://journals.cambridge.org/PLA

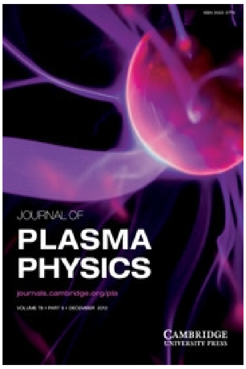

Additional services for ***Journal of Plasma Physics:***

Email alerts: Click here
Subscriptions: Click here
Commercial reprints: Click here
Terms of use : Click here

Rotating magnetohydrodynamics

X. Shan and D. Montgomery

Journal of Plasma Physics / Volume 52 / Issue 01 / August 1994, pp 113 - 128
DOI: 10.1017/S0022377800017803, Published online: 13 March 2009

Link to this article: http://journals.cambridge.org/abstract_S0022377800017803

How to cite this article:
X. Shan and D. Montgomery (1994). Rotating magnetohydrodynamics. Journal of Plasma Physics, 52, pp 113-128 doi:10.1017/S0022377800017803

Request Permissions : Click here

CAMBRIDGE JOURNALS

Downloaded from http://journals.cambridge.org/PLA, IP address: 139.184.30.131 on 10 Dec 2012

J. Plasma Physics (1994), *vol.* 52, *part* 1, *pp.* 113–128

Copyright © 1994 Cambridge University Press

Rotating magnetohydrodynamics

By X. SHAN AND D. MONTGOMERY

Department of Physics and Astronomy, Dartmouth College, Hanover,
New Hampshire 03755-3528, U.S.A.

(Received 25 April 1994)

It is shown that rotation of a periodic column of magnetohydrodynamic fluid can be stabilized against current-driven instabilities by rotation. The rotation is considered as resulting from a slight departure from overall charge neutrality, and is braked by wall friction (loss of angular momentum to the cylinder wall). Both effects are modelled phenomenologically in the equation of motion, and the emphasis is on their bulk dynamic effects rather their microscopic kinetic theory origins. Much as rotation is known to stabilize a Navier–Stokes fluid against transverse displacements, it is shown that sufficient rotation will suppress the helical vortices and helical deformations of the current channel that are known to result when the axial current in the column exceeds its stability threshold.

---

1. Introduction

When a Navier–Stokes fluid is 'spun up', or rotated at a fixed angular velocity, the fluid elements acquire an effective elastic binding to their steady-state positions in the two dimensions perpendicular to the axis of rotation. Small oscillations thereby become possible that were not possible for a non-rotating fluid (see e.g. Batchelor 1967; Greenspan 1968; Acheson 1990). There is stabilization against small displacements of the fluid elements by virtue of the rotation. The purpose of this paper is to present evidence that a related stabilization through rotation may occur in magnetohydrodynamics (MHD).

Usually, rotation of a Navier–Stokes fluid occurs because of the rotation of a material surface with which it is in contact. The surface might be a cylindrical container, for example, or perhaps the bottom of the ocean. Magnetofluids may acquire rotation velocities through less direct means. A small departure from charge neutrality, for instance, may result in a radially outward or inward electric field from Gauss's law, in cylindrical geometry. If an externally supported axial magnetic field is present, the resulting $\mathbf{E}\times\mathbf{B}$ particle drift can produce an azimuthal fluid velocity. Rotation of plasmas in 'Q machines' has been so interpreted since the 1960s. Chen & Montgomery (1993) have recently treated the case of a slightly non-neutral magnetized plasma in an axial magnetic field in thermal equilibrium, and have identified a rigidly rotating axisymmetric state as the thermal equilibrium one in the presence of perfectly smooth impenetrable walls in a periodic cylinder geometry. The charge excess or deficiency was shown to be concentrated in a boundary layer near the cylinder wall. However, the necessarily complex microscopic interaction of real plasmas with their boundaries (limiters or divertors, for example, in the case of tokamak confinement) will make the rigidly rotating, or 'spun-up', profile an inadequate description.

Both the plasma/wall interaction and the radial distribution of a small net charge in a magnetized plasma are inherently kinetic processes, and their inclusion in a self-contained MHD description will necessarily have a somewhat *ad hoc* phenomenological quality. Nevertheless, it seems likely, because of their complexity, that such a phenomenological inclusion in MHD is the only possibility for assessing their effects on fully general, time-dependent, nonlinear behaviour.

An experimental situation that led to the investigations reported here (but otherwise not connected to it in detail) is the so-called 'L-to-H transition' in tokamaks. 'L' stands for 'low' and 'H' for 'high', and these refer to the degree of confinement and quiescence in the plasma. An apparently spontaneous transition was sometimes observed in tokamaks (see e.g. ASDEX team 1989) to a regime (the 'H mode') with superior confinement properties. The desirability of 'H-mode' operation has generated a large literature of further experiments and proposed explanations (an on-line literature search of the references since 1988 returns about 150 publications; a useful review by Burrell *et al.* (1992) contains over 80 citations). The phenomenon is complex, and exhibits a morphology that varies from machine to machine. A single detailed explanation encompassing all of the observed phenomena seems increasingly unlikely. We focus here not on the experimental L/H transition as such, but rather on an MHD problem that one subset of the L/H measurements has suggested: stabilization through rotation.

An early observation of the L/H transition was that it was often accompanied by the appearance of a flow velocity, often but not always in the azimuthal ('poloidal') direction. A 'shear' was often inferred in the velocity field (i.e. a departure from a rigid rotation profile) from radial electric field measurements and their interpretation in terms of an $\mathbf{E}\times\mathbf{B}$ drift. Taylor *et al.* (1990; see also Tynan *et al.* 1992) showed explicitly how an electrostatically produced poloidal rotation velocity could trigger the H-mode transition. Theoretical interpretations of this observation have been diverse and full of puzzles and controversy.

The focus here is on what we believe to be a generic MHD result suggested by some of these observations: that stabilization of a current-carrying magnetofluid can result from poloidal rotation (of whatever origin), in much the same way that rotation is known to stabilize a Navier–Stokes fluid. The method is numerical solution of the MHD equations, suitably modified to include rotation and wall friction. A fully three-dimensional MHD spectral code (previously described in detail in Shan, Montgomery & Chen 1991; Shan & Montgomery 1993*a*, *b*; Montgomery 1993) can be readily adapted to include the rotation and wall friction. The two modifications to MHD are described in §2, which also summarizes previous results obtained from the code for the non-rotating case. Section 3 is a brief summary of the numerical method, and can be skipped by a reader who is interested only in the results. Essentially no new numerical complications result from the modifications necessary in the numerics. Section 4 is devoted largely to the changes, from the previously published results, to which the rotation and wall friction lead. Section 5 is a brief summary, and identifies possible future directions.

2. Rotating MHD with wall friction

We write the MHD equation of motion in a standard set of dimensionless ('Alfvénic') units. Only the first and last terms on the right-hand side are in any way non-standard:

$$\frac{\partial \mathbf{v}}{\partial t}+\mathbf{v}.\nabla\mathbf{v} = -\frac{\mathbf{v}-\mathbf{v}_0}{\tau}+\mathbf{j}\times\mathbf{B}-\nabla p+\nu\nabla^2\mathbf{v}-\lambda(r)\,\mathbf{v}. \tag{1}$$

Here $\mathbf{v} = \mathbf{v}(\mathbf{x}, t)$ is the fluid velocity, assumed solenoidal; the mass density of the magnetofluid is assumed to remain spatially uniform. The mechanical pressure is p, the magnetic field is $\mathbf{B}$, $\mathbf{j} = \nabla\times\mathbf{B}$ is the current density, and ν is the kinematic viscosity. The function $\mathbf{v}_0$ is a poloidal (azimuthal) rotation velocity, and is assumed to be given as a function of position. τ is a spin-up time, also assumed to be given. For $\mathbf{v}_0$, we have typically chosen $\mathbf{v}_0 = \frac{1}{2}r\omega_0\,\hat{\mathbf{e}}_\phi$ in cylindrical co-ordinates (r, ϕ, z), with ω_0 a uniform axial vorticity. τ is also assumed to be a uniform constant. We have experimented with assigning radial variation to $\mathbf{v}_0$ and τ, but without a noticeably significant change in the results. $\lambda = \lambda(r)$ is a phenomenological friction coefficient, which only becomes significant in magnitude near the radius of the cylinder, which lies at $r = a$. This last term in (1) models what are complicated, situation-dependent kinetic processes involving loss of momentum and angular momentum to whatever mechanical element (limiter, divertor) is being idealized at $r = a$. Without the $-\lambda(r)\,\mathbf{v}$ term, the first term on the right-hand side of (1) would by itself have the effect of 'spinning up' the magnetofluid to the azimuthal velocity $\mathbf{v}_0$ in a time of order τ. It is understood to model the effects of non-neutrality in a way that consciously oversimplifies the kinetic processes involved in the interests of having a tractable representation of their effects in bulk MHD. The wall friction term frustrates the attempt to achieve rigid rotation, and imposes a 'shear', or radial gradient in the axial vorticity, in the region where the first and last terms on the right-hand side of (1) compete.

The magnetic field is advanced by Faraday's law,

$$\frac{\partial \mathbf{B}}{\partial t} = -\nabla\times\mathbf{E}, \tag{2}$$

where $\mathbf{E}$ is the electric field. Ohm's law, in the form

$$\mathbf{E}+\mathbf{v}\times\mathbf{B} = \eta\mathbf{j}, \tag{3}$$

is assumed to apply. The magnetic diffusivity η is assumed to be a given function of the radius r that increases steeply towards $r = a$, reflecting the strong dependence of electrical conductivity on temperature. The viscosity ν, however, is treated as a uniform constant.

The geometry considered is a straight cylinder of length L_z, with periodically identified ends – the lone concession to the toroidal geometry in which the L/H transition has typically been studied. An axial magnetic flux with mean magnetic field $\mathbf{B}_0$ is assumed to be supported externally. An applied electric field $\mathbf{E} = E_0\,\hat{\mathbf{e}}_z$ is assumed to drive a current in the axial direction. In the absence of any mechanical activity ($\mathbf{v} = 0$) or spin-up ($\mathbf{v}_0 = 0$), the steady-state current density is $\mathbf{j} = E_0 \hat{\mathbf{e}}_z/\eta$ and the azimuthal (poloidal) magnetic field is

$$B_\phi(r) = (2\pi r)^{-1} \int \frac{E_0}{\eta(r)} r\, dr\, d\phi,$$

where the surface integral is over the area of a circular cross-section of radius a. The pinch ratio is defined as $\Theta_0 = B_\phi(a)/B_0$, and the Hartmann number (evaluated at $r = 0$) is $H_0 = aC_A/(\eta\nu)^{\frac{1}{2}}$, where C_A is the toroidal Alfvén speed (H_0 is just $B_0/(\eta\nu)^{\frac{1}{2}}$ in these dimensionless units). It has been shown previously (Montgomery 1992; Shan & Montgomery 1993*a*) that Θ_0 and H_0 govern the linear stability threshold of any axisymmetric, non-rotating state. Θ_0 may also be expressed in terms of the 'safety factor' $q(a)$ evaluated at $r = a$:

$$\Theta_0 = \frac{2\pi a}{L_z q(a)}.$$

The wall at $r = a$ is imagined as a rigid perfect conductor, mechanically impenetrable, and coated with a thin layer of insulating dielectric at $r = a$. The boundary conditions implied by this are that at $r = a$, $\mathbf{j}.\hat{\mathbf{n}} = 0$, $\mathbf{B}.\hat{\mathbf{n}} = 0$, $\mathbf{v}.\hat{\mathbf{n}} = 0$, where $\hat{\mathbf{n}} = \hat{\mathbf{e}}_r$ is the unit normal to the wall. A second mechanical boundary condition may be chosen, and a classical fluid-dynamical perspective might suggest either $\mathbf{v} \times \hat{\mathbf{n}} = 0$ ('no slip'), or $\hat{\mathbf{n}} \times \boldsymbol{\sigma}.\hat{\mathbf{n}} = 0$, where $\boldsymbol{\sigma}$ is the viscous stress tensor (a 'stress-free' wall). With the numerical method used, both these boundary conditions turn out to be quite difficult to implement, and probably represent no better the complex plasma/wall interaction than the one we do choose: $\boldsymbol{\omega}.\hat{\mathbf{n}} = 0$, where $\boldsymbol{\omega} = \nabla \times \mathbf{v}$ is the vorticity. The condition $\boldsymbol{\omega}.\hat{\mathbf{n}} = 0$ is implied by, but does not imply, no-slip boundary conditions. The wall drag will be simply accounted for by the term $-\lambda(r)\,\mathbf{v}$ in (1). $\lambda(r)$ becomes significant only near $r = a$.

Previous publications (Montgomery, Phillips & Theobald 1989; Chen, Shan & Montgomery 1990; Agim & Montgomery 1991; Shan *et al.* 1991; Montgomery 1992, 1993; Shan & Montgomery 1993*a*, *b*) have explored in some detail the dynamical events that occur as E_0 and thus Θ_0 are raised from zero. A linear stability boundary in the (H_0, Θ_0) plane can be sharply identified for a given $\eta(r)$. The linear stability analysis can be given analytically for a uniform η, but requires numerical computation for a spatially variable one (Shan & Montgomery 1993*b*). As long as Θ_0 remains below the value where any normal mode grows temporally, arbitrary initial perturbations damp away owing to resistivity and viscosity, and the magnetofluid returns to its axisymmetric, zero-flow, steady state.

When Θ_0 is raised just above its (calculable) stability threshold, the steady state bifurcates. The preferred branch (as revealed by dynamical computation) is no longer axisymmetric, but helically symmetric. The MHD fields are additive combinations of the axisymmetric steady-state fields and their linearly unstable eigenmodes, plus small higher-order contributions from their interactions. In this regime an arbitrarily perturbed initial state will relax to a time-independent steady state with helical symmetry and a lower energy dissipation rate (at fixed E_0) than the corresponding axisymmetric resistive equilibrium, which is now unstable.

Further increases in E_0 lead to other interesting transitions, not yet fully mapped out. For example, the poloidal and toroidal mode numbers (m and n)

that characterize the helical state may change (the unstable eigenmodes vary as $\exp(im\phi - i2\pi nz/L_z)$). 'Multi-mode' states, with more than one m/n ratio present, may be excited, and may acquire a persistent quasi-periodic time dependence. Eventually, as E_0 is increased further, fully developed MHD turbulence sets in, and has been both difficult to characterize and difficult to compute. Our numerical methods are not adequate to explore the fully turbulent state.

In summary, as E_0 is raised, an increasing level of mechanical and magnetic MHD activity sets in, and at each transition the fields seem less likely to be ones that would confine a plasma well or minimize its transport. The analogy with hydrodynamic pipe flow, as the pressure drop and Reynolds number are raised, is non-trivial, and the observed MHD behaviour is of a piece with hydrodynamic scenarios as viscous flows are subjected to steeper pressure gradients.

The question of interest here is taken to be 'What possibilities exist for the two new terms in (1) to suppress this MHD activity, and what levels of rotation ω_0 are required?' How does one characterize the rotating state? Easy and relatively superficial answers, for the case of uniform η and $\lambda = 0$, can be given analytically (Montgomery, Chen & Shan 1991), but for the case of radially increasing η and non-zero λ numerical computation is required. We now give a brief summary of the numerical method before turning to the results to which it leads.

3. Numerical method

The code has been described elsewhere in considerable detail (Shan *et al.* 1991; Shan & Montgomery 1993*a*); this section is a brief description of its operation. All fields are expanded in Chandrasekhar–Kendall functions, or orthonormal eigenfunctions of the curl. These start from any solution of the scalar wave equation

$$(\nabla^2 + \lambda^2)\psi = 0, \tag{4}$$

and are defined, before normalization, by the expression

$$\mathbf{A} = \lambda \nabla \times \hat{\mathbf{e}}\psi + \nabla \times (\nabla \times \hat{\mathbf{e}}\psi), \tag{5}$$

where $\hat{\mathbf{e}}$ is a constant unit vector. It is easy to show, using (4), that $\nabla \times \mathbf{A} = \lambda \mathbf{A}$.

For the case of the periodic cylinder, the appropriate choice of $\hat{\mathbf{e}}$ is $\hat{\mathbf{e}}_z$, and

$$\psi = \psi_{nmq} = J_m(\gamma_{nmq} r)\exp(im\phi - ik_n z).$$

Here $m = 0, \pm 1, \pm 2, \ldots$; $n = 0, \pm 1, \pm 2, \ldots$; $k_n = 2\pi n/L_z$; $q = 1, 2, \ldots$; and $\gamma_{nmq}^2 + k_n^2 = \lambda_{nmq}^2$ defines λ_{nmq} (both signs allowed). Thus the $\mathbf{A}_{nmq}$ are indexed by three integers, and may be normalized so that

$$(\mathbf{A}_{nmq}, \mathbf{A}_{n'm'q'}) = \frac{1}{V}\int \mathbf{A}_{nmq}^* . \mathbf{A}_{n'm'q'}\, r\,dr\,d\phi\,dz = \delta_{nn'}\delta_{mm'}\delta_{qq'}, \tag{6}$$

where the volume integral runs over the interior of the periodic cylinder, and $V = \pi a^2 L_z$. The γ_{nmq} are determined by imposing the boundary condition $\mathbf{A}_{nmq} . \hat{\mathbf{e}}_r = 0$ at $r = a$, for all m, n, q such that $m^2 + n^2 > 0$. For $m = n = 0$ the γ_{00q} are determined by demanding that $\int \mathbf{A}_{00q} . \hat{\mathbf{e}}_z\, r\,dr\,d\phi = 0$ when integrated over a cross-section of the cylinder. This makes all the $\mathbf{A}_{00q}$ 'fluxless', and, since one is interested in expanding fields such as $\mathbf{j}$ and $\mathbf{B}$ that have non-zero axial fluxes, the $\mathbf{A}_{00q}$ must be supplemented by a function $\mathbf{A}_0(r)$ with a finite flux, orthogonalized to all the retained $\mathbf{A}_{00q}$, by the Schmidt orthogonalization procedure (for details see Shan *et al.* 1991). All the fields are then expanded in the $\mathbf{A}_{nmq}$ and $\mathbf{A}_0(r)$; for example,

$$\mathbf{B} = j_0 \mathbf{A}_0 + B_0 \hat{\mathbf{e}}_z + \sum_{nmq} \xi^B_{nmq} \mathbf{A}_{nmq}, \tag{7}$$

$$\mathbf{v} = \omega_0 \mathbf{A}_0 + v_0 \hat{\mathbf{e}}_z + \sum_{nmq} \xi^V_{nmq} \mathbf{A}_{nmq}. \tag{8}$$

The ξ^B_{nmq}, ξ^V_{nmq}, j_0 and ω_0 are time-dependent complex expansion coefficients, and serve as the dynamical variables of the problem.

The expansions (7) and (8) and their curls are substituted into (1)–(3). Then inner products are taken one at a time with the expansion functions, and (6) permits ordinary first-order differential equations to be extracted in the usual fashion of a Galerkin approximation. These have the generic form

$$\frac{dX_\alpha}{dt} = \sum_\beta C_{\alpha\beta} X_\beta + \sum_{\beta\gamma} C_{\alpha\beta\gamma} X_\beta X_\gamma + E_\alpha, \tag{9}$$

where X_α is an element of a column vector whose elements are all the real and imaginary parts of the ξ^B_{nmq}, ξ^V_{nmq}, j_0 and ω_0. The coupling coefficients $C_{\alpha\beta}$ and $C_{\alpha\beta\gamma}$ involve integrals of Bessel functions, and are stored as a table. The E_α stand for any external forcing terms that may be present (in this case the effect of applied axial electric field). The number of independent X_α retained may typically be about 2000, and they are advanced according to (9) by a time-stepping routine appropriate to 'stiff' ODEs. The method converges rapidly (i.e. the answers become independent of the further addition of expansion functions) for situations not too far above the stability threshold in Θ_0, but does not converge well for fully turbulent cases.

The time advancement takes place entirely in spectral space. Only when it is necessary to construct configuration-space graphics it is required to reconstruct the fields as functions of $\mathbf{x}$ from (7) and (8). The reason the code converges rapidly, when it does, is that the expansion functions are close to the linear normal modes of the system. They are exactly the linear normal modes for the case of uniform η, and the m and n indices are still 'good quantum numbers' even when η depends upon r. Often, a numerical code does not have the luxury of a set of expansion functions that individually are already quite close to the linear eigenfunctions of the physical problem, including the boundary conditions. For example, in the case of plane shear flows, the Orr–Sommerfeld eigenfunctions are far from the Fourier–Chebyshev expansion functions sometimes used to decompose them (see e.g. Canuto *et al.* 1988).

The two new terms in (1) are readily accommodated in the numerical scheme, and essentially no innovations are required. We turn now to the differences in the dynamical behaviour that the new terms induce in the near-threshold dynamical behaviour, relative to that behaviour in the absence of rotation and wall friction, as previously described.

4. Rotation damping of helical MHD activity

In order to compare the rotating MHD results with the non-rotating ones, we pick again the resistivity profile used by Carreras *et al.* (1980) and Hicks *et al.* (1981) in studying 'tearing-mode' activity. This was used earlier by us (Shan &

	B_0	ν	η_0	H_0	E_0	Θ_0	Λ_*	r_*
Run I	4	10^{-4}	10^{-4}	40000	$1{\cdot}39\times10^{-4}$	0·052	10	0·9
Run II	2	2×10^{-4}	10^{-4}	14142	$1{\cdot}16\times10^{-4}$	0·11	4	0·7
Run III	2	2×10^{-4}	10^{-4}	14142	$1{\cdot}16\times10^{-4}$	0·11	10	0.9

TABLE 1. Parameters of the runs (η_0 and H_0 are evaluated on axis)

Montgomery 1993*a*, *b*) in the investigation of the dependence of MHD activity upon the on-axis Hartmann number. For the magnetic diffusivity profile, we take

$$\eta(r) = \eta_0\left[1+\left(\frac{r}{r_0}\right)^{2\Lambda}\right]^{1+1/\Lambda},$$

with $a = 1{\cdot}0$, $r_0 = 0{\cdot}6$, aspect ratio $L_z/2\pi a = 2{\cdot}5$ and $\Lambda = 4{\cdot}0$. The steady-state current profile is

$$j_z(r) = E_0/\eta(r).$$

The stability boundary in the plane has previously been determined and exhibited (Shan & Montgomery 1993*b*). The safety factor profile

$$q(r) = q(0)\left[1+\left(\frac{r}{r_0}\right)^{2\Lambda}\right]^{1/\Lambda}$$

has the value $q(0) = 4\pi aB_0\eta_0/E_0L_z$ on axis, is relatively flat out to the neighbourhood of $r = r_0$, and then rises more abruptly toward the wall $r = a$. For the wall friction coefficient $\lambda(r)$, we must also make a definite choice, and we pick the function

$$\lambda(r) = \tau^{-1}\left[1+\left(\frac{r}{r_*}\right)^{2\Lambda_*}\right]^{1+1/\Lambda_*} - \tau^{-1},$$

with Λ_* and r_* as constants to be specified. This function is almost zero in the interior, and becomes significant only at the edge of the cylinder, $r > r_*$. The viscosity is treated as a uniform constant throughout. (We do not inquire here into how the net plasma charge arises or distributes itself.) The reciprocal of the spin-up time τ^{-1} is allowed to go from zero to a finite value of 0·01 at the time it is desired to begin studying the effects of rotation. The angular rotation rate $\frac{1}{2}\omega_0$ may be changed at times of choice when it is desired to study the effect of increasing the rotation rate. All times are measured in Alfvén transit times of unit distance and unit magnetic field strength.

To illustrate our results, we have made three runs with the code, hereafter called runs I, II and III. Table 1 summarizes the various parameters used in these three runs. All these calculations are started with the trivial equilibrium $\mathbf{v} = 0$ and $\mathbf{j} = E_0\hat{\mathbf{e}}_z/\eta(r)$, plus small-amplitude (of order 10^{-4} in amplitude) noise randomly distributed amongst all the expansion functions $\mathbf{A}_{nmq}$. This trivial equilibrium is unstable with all three sets of parameters given in Table 1. The two new terms in (1) are turned off initially until the helical unstable modes grow and saturate. We then study the effects of rotation on the helical MHD

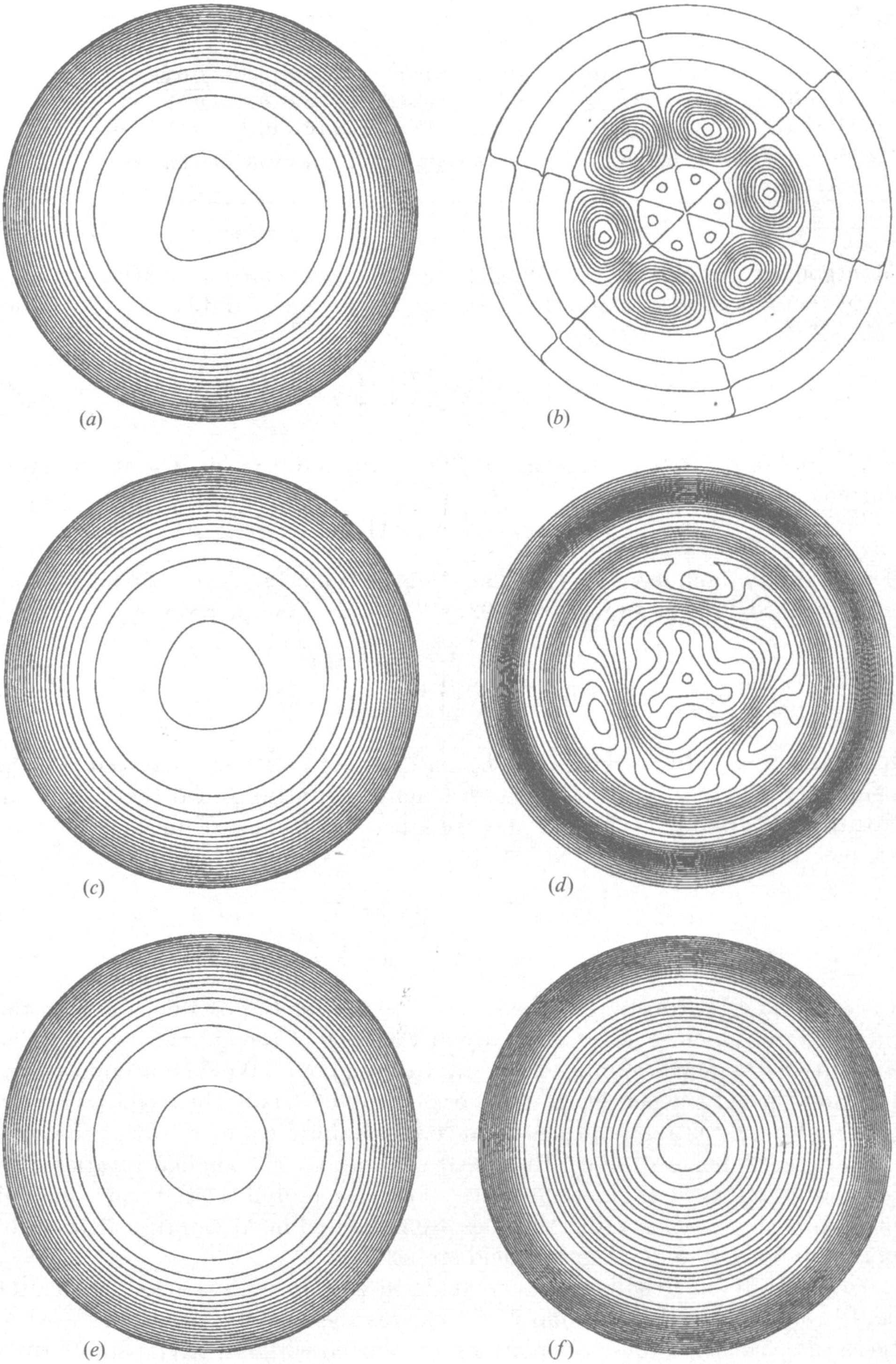

FIGURE 1. Contours are intersections of magnetic surfaces (a, c, e) and vorticity field line surfaces (b, d, f) with the plane $z = 0$ at three different times for run I: (a) and (b) are at $t = 600$, after the helical MHD activity has developed and at the instant the rotation is turned on; (c) and (d) are at $t = 700$; (e) and (f) are at $t = 1200$, at which time the helical MHD activity has been almost totally suppressed. Times are in Alfvén transit times of unit magnetic field and unit distance ($a = 1$).

activity by turning on the wall friction effect and raising the rotational driving term incrementally.

For run I the parameters are barely on the unstable side of the stability boundary of the $m/n = 3/1$ mode in the (Θ_0, H_0) plane. Small initial random noise is allowed to amplify, and, as before, the magnetofluid goes into a helical steady state with stationary paired helical vortices with $m/n = 3/1$. Since this steady state is purely helically symmetric, well-defined flux surfaces exist for the quantities $\mathbf{B}$, $\mathbf{j}$, $\mathbf{v}$ and ω. Figure 1 (*a*) is a computer-drawn cross-section of the magnetic surfaces that characterize this steady state, and figure 1 (*b*) is a cross-section of the flux surfaces of the steady-state vorticity, both at time $t = 600$. At time $t = 600$, τ^{-1} is allowed to take on the value 0·01, with $\omega_0 = 0{\cdot}2$. By $t = 700$ (figures 1*c*, *d*), the departure from axisymmetry in these two quantities has been noticeably suppressed, and by $t = 1200$ (figures 1*e*, *f*), a nearly axisymmetric state has been achieved. This suppression process of the helical deformation can be seen more clearly in the modal energy plots shown in figure 2, where each line in (*a*) and (*b*) is the time history of the kinetic or magnetic energy of the helical modes with a specific m/n ratio, i.e. the same helical symmetry. From the two contour plots of ω_z shown in figure 3, at $t = 550$ and 1000, it can be seen that a 'shear layer', or layer of steep radial gradient in the axial vorticity has developed just inside the wall $r = a = 1$ at $t = 1000$, at which time the axisymmetry has been recovered almost totally. The behaviour illustrated in figures 1–3 is typical of what happens if sufficient rotation is applied to stabilize the magnetofluid completely against the appearance of the helical states. The azimuthal velocity profile at $t = 1200$ is shown in figure 4. In terms of the toroidal Alfvén speed, the amount of rotation applied in this case to make the axisymmetry disappear corresponds to a maximum rotation speed of 0·03 times the Alfvén speed. Note that without the wall friction term in (1), the radial dependence of the azimuthal velocity would be linear. The boundary layer begins just above $r_* = 0{\cdot}7$ here, the choice of which is optional.

In run I we have demonstrated the suppression of a purely helically symmetric stationary mode by the rotation of the magnetofluid. More generally, the rotation will make the magnetofluid inside the cylinder more stable against any perturbations, even when the helical MHD activity was not stationary. We have previously shown that when either Θ_0 or H_0 is raised to sufficiently higher values, the magnetofluid will bifurcate into some more and more complex states. We shall demonstrate next in run II that the rotation of the magnetofluid has an effect opposite to that of increasing Θ_0 and H_0. The parameters for run II put it well inside the unstable region of both 2/1 and 3/2 modes in the (θ_0, H_0) plane. (This corresponds to what was called run 3 in Shan & Montgomery (1993*b*).) As before, in the initial stage, when both the rotational driving force and the wall friction are turned off, the unstable modes grow out of the random perturbation and form a multi-mode state with $m/n = 2/1$ and 3/2 being the largest modes. We then turn on the wall friction and increase ω_0 gradually as a sequence of step functions. The gradual suppression of the helical perturbations is most apparent in the time history plot of the modal kinetic and magnetic energies of the helical perturbations shown in figure 5. As the rotation rate is increased, the magnetofluid becomes more and more quiescent: from the three-dimensional state to two-dimensional helically symmetric state, and eventually to the one-dimensional axisymmetric state. Since in states involving

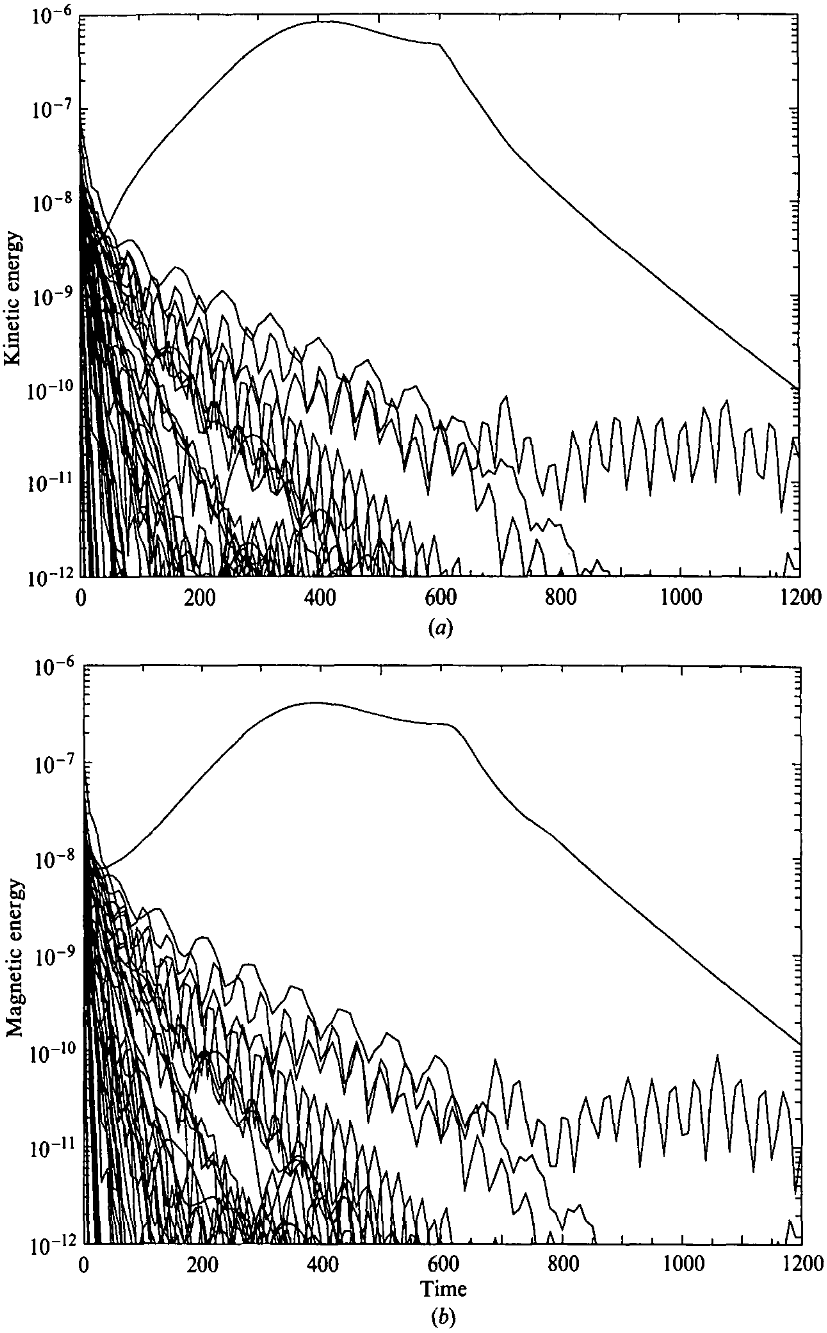

FIGURE 2. Time histories of the modal kinetic energies (*a*) and modal magnetic energies (*b*) for run I. The traces are for all modes with given m/n, summed over q.

many different m/n ratios the existence of any flux surfaces is impossible to assert, we show in figure 6 a series of contours of the axial vorticity field ω_z at typical times (*a*) 300, (*b*) 900, (*c*) 1500, (*d*) 2100, (*e*) 2700 and (*f*) 3300. The transition to a helically symmetric state (*d*, *e*) and finally to an axisymmetric equilibrium (*f*) is again apparent in this series of plots.

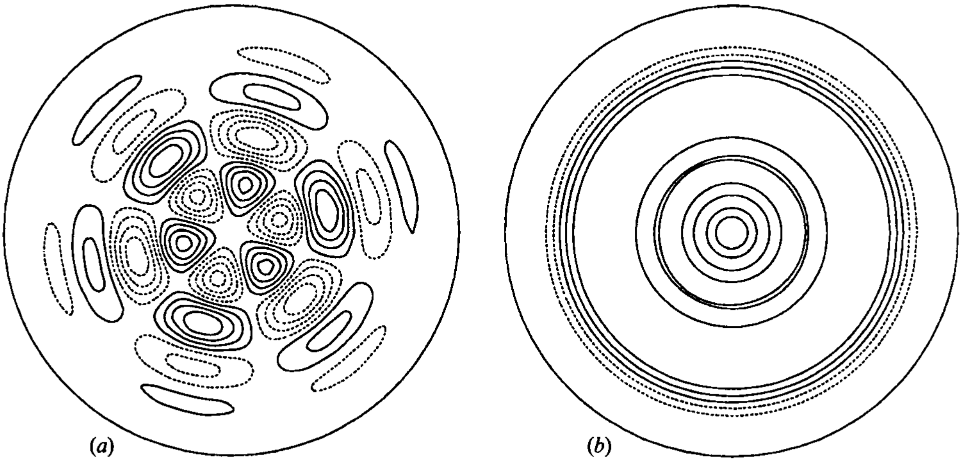

FIGURE 3. Contours of constant axial vorticity component in the plane $z = 0$ at times $t = 550$ (*a*) and $t = 1000$ (*b*) for run I.

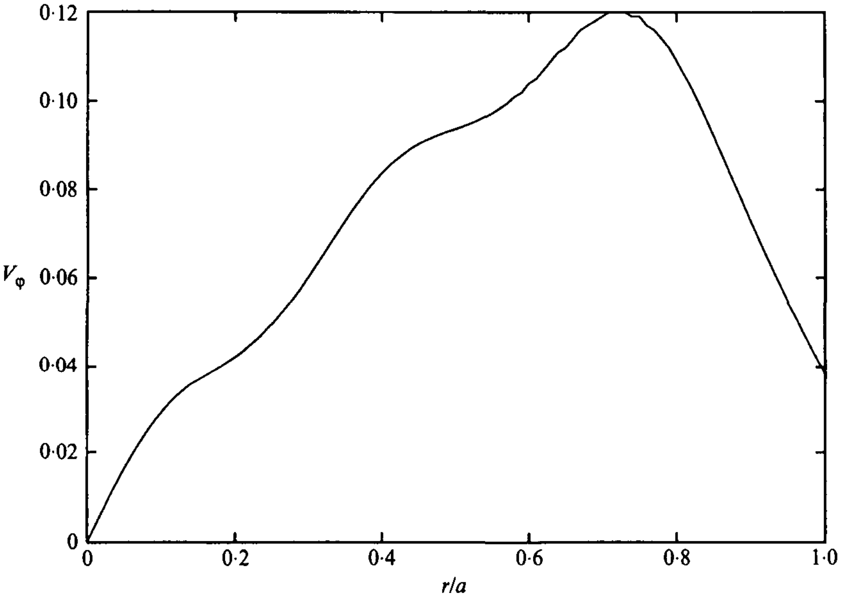

FIGURE 4. Azimuthal velocity field averaged over a cylindrical surface of radius r, plotted as a function of r, for run I at $t = 1200$. The maximum rotation velocity is about 0·03 of a toroidal Alfvén speed.

The third run would otherwise be identical to run II, except that here we employed a thinner wall friction layer by choosing different Λ_* and r_*. An interesting feature of this run is the sawtooth-like oscillation in the less-dominant m/n ratios when the rotation induces a transition from the 'mixed-mode' state to the helically symmetric state, as can be seen in the modal energy plot shown in figure 7. This oscillation, which occurs between about $t = 1000$ and $t = 3500$, is a limit-cycle solution of the dynamical system (9), and has been reported in previous calculations (Shan & Montgomery 1993*b*). Still further

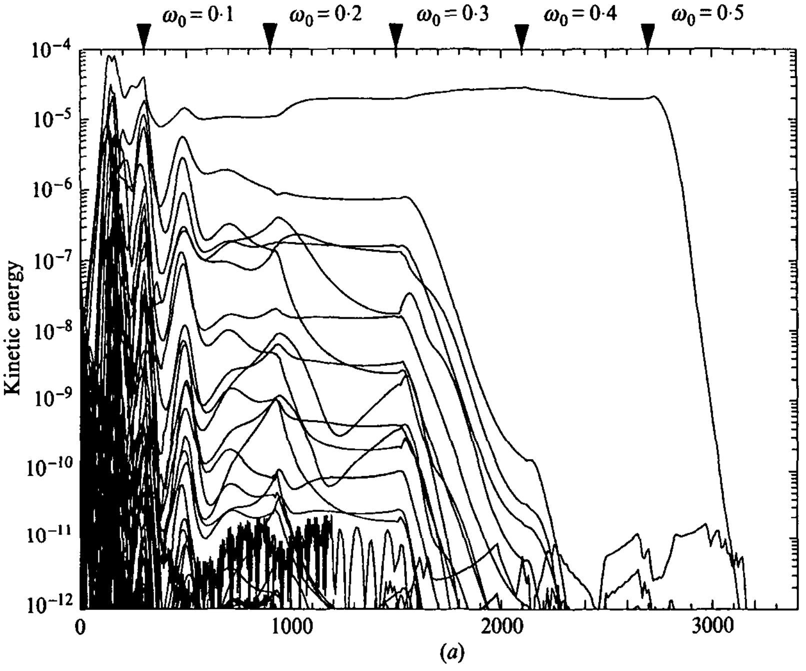

(*a*)

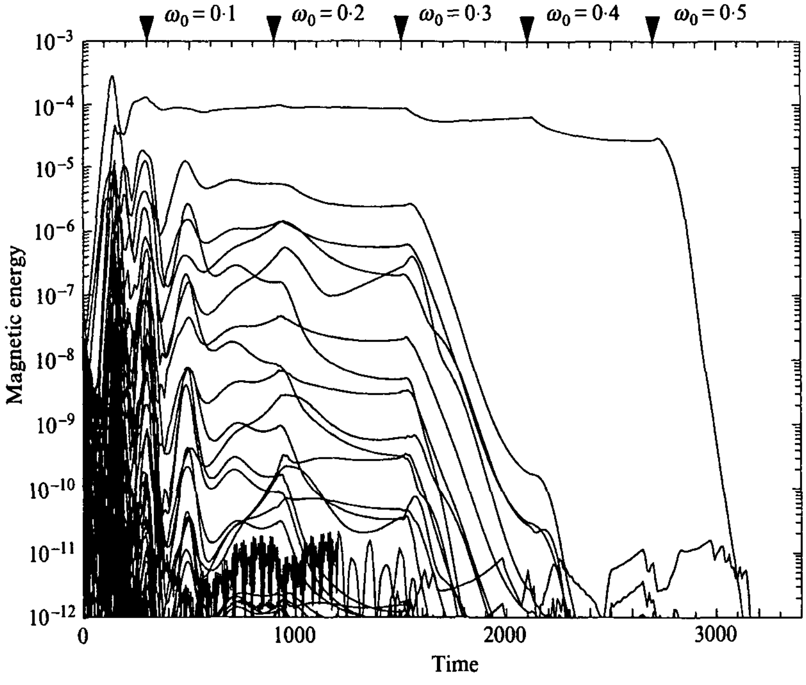

(*b*)

FIGURE 5. Time histories for run II of the kinetic modal energies (*a*) and magnetic modal energies (*b*), with all modes corresponding to a singe m/n combined. For this run, the rotation rate is stepped up incrementally from zero, at the instants indicated by the arrows at the top of the graph. The values of axial vorticity turned on are printed just after the arrows.

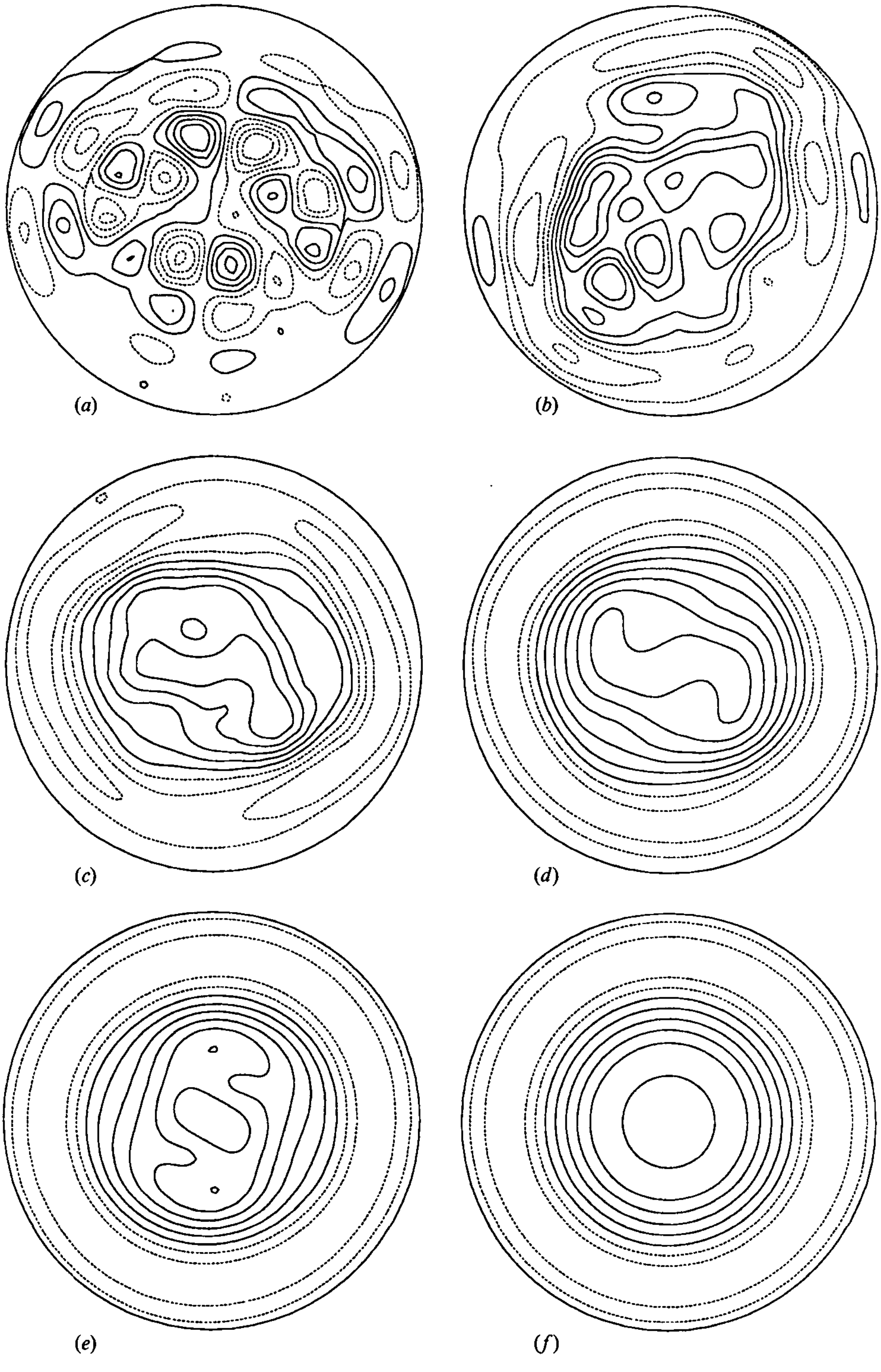

FIGURE 6. Contours of constant axial vorticity in the plane $z = 0$ at times $t = 300$ (*a*), 900 (*b*), 1500 (*c*), 2100 (*d*), 2700 (*e*) and 3300 (*f*) for run II. Because this is a mixed state with several m/n ratios present during the greatest dynamical activity, no magnetic surfaces can be drawn.

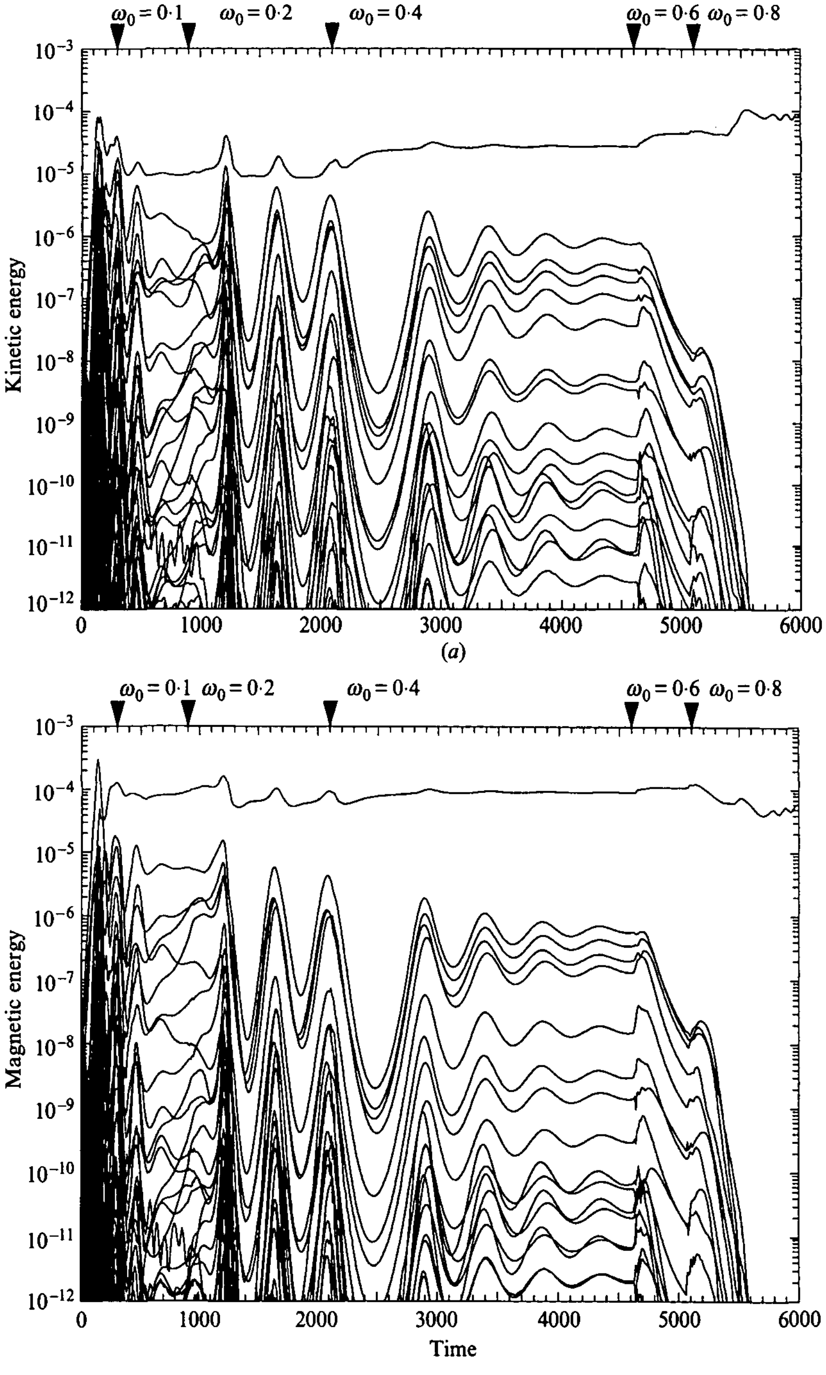

(b)

FIGURE 7. Kinetic modal energies (*a*) and magnetic modal energies (*b*) for run III. This run is for the same plasma conditions as run II, except that a thinner wall friction layer has been induced by choosing a value of $r_* = 0{\cdot}9$ and $\Lambda_* = 10$. The rotation is again increased incrementally, with the times indicated by arrows at the top of the graph, and values of the axial rotation vorticity ω_0 printed immediately to the right of the arrows.

increases in the rotation rate would lead to the total disappearance of all the helical contributions. The single-m/n state might be called the 'MHD L mode'. The MHD system oscillates around the helically symmetric equilibrium, in a way quite similar to what has been observed in experiments by Zohm *et al.* (1994) during an L–H transition.

5. Discussion and possible extensions

We consider it noteworthy that rotation seems to have a generic effect of stabilizing current-driven MHD activity near its stability threshold. It is perhaps significant that the layer of strong velocity shear, visible for example in figure 3(*b*), has appeared as a consequence of the combined effects of the non-charge-neutral rotation and the boundary friction, rather than as a cause of the rotation, as has sometimes been suggested. The modelling done for stepping outside the MHD framework to get the $\mathbf{E}\times\mathbf{B}$ rotation due to net charge and the wall interaction is crude, and it may be a very long time before microscopic kinetic theory will advance to the point at which the adequacy of the model terms in (1) can be tested. Nevertheless, the experimental message is clear: rotation is a good thing from the point of view of bulk MHD stabilization. Since experimental techniques are available for inducing rotation (by, for example, the introduction of electrons into the column, as in Taylor *et al.* 1989), it would appear to be desirable to study empirically the effects of making confined plasmas rotate in a systematic fashion.

The limitations to uniform density and incompressible flow, the absence of Braginskii viscous stress tensors (particularly the 'ion-parallel' part) and the lack of a local temperature dependence for the conductivity are all severe limitations, the lifting of which would be desirable. However, none of them is trivial.

We are grateful to Dr Hudong Chen for helpful discussions. This work was supported in part by U.S. Department of Energy Grant DE-FGO2-85ER53194, subcontract 9-XA3-1416E-1 from Los Alamos National Laboratory, and NASA Grant NAG-W-710.

REFERENCES

Acheson, D. J. 1990 *Elementary Fluid Dynamics*. Clarendon.

Agim, Y. Z. & Montgomery, D. 1991 *Plasma Phys. Contr. Fusion* **33**, 881.

ASDEX Team 1989 *Nucl. Fusion* **29**, 1959.

Batchelor, G. K. 1967 *An Introduction to Fluid Dynamics*. Cambridge University Press.

Burrell, K. H., Carlstrom, T. N., Doyle, E. J., Finkenthal, D., Gohil, P., Groebner, R. J., Hillis, D. L., Kim, J., Matsumoto, H., Moyer, R. A., Osborne, T. H., Rettig, C. L., Peebles, W. A., Rhodes, T. L., St John, H., Stambaugh, R. D., Wade, M. R. & Watkins, J. G. 1992 *Plasma Phys. Contr. Fusion* **34**, 1859.

Canuto, C., Hussaini, M. Y., Quarteroni, A. & Zang, T. A. 1988 *Spectral Methods in Fluid Dynamics*. Springer.

Carreras, B. A., Hicks, H. R., Holmes, J. A. & Waddell, B. V. 1980 *Phys. Fluids* **23**, 1811.

Chen, H. & Montgomery, D. 1993 *J. Plasma Phys.* **49**, 341.

Chen, H., Shan, X. & Montgomery, D. 1990 *Phys. Rev.* A **42**, 6158.

Greenspan, H. P. 1968 *The Theory of Rotating Fluids*. Cambridge University Press.

Hicks, H. R., Carreras, B. A., Holmes, J. A., Lee, D. K. & Waddell, B. V. 1981 *J. Comp. Phys.* **44**, 46.

Montgomery, D. 1992 *Plasma Phys. Contr. Fusion* **34**, 1157.

Montgomery, D. 1993 *Plasma Phys. Contr. Fusion* **35**, B105.

Montgomery, D., Chen, H. & Shan, X. 1991 *Plasma Phys. Contr. Fusion* **33**, 1871.

Montgomery, D., Phillips, L. & Theobald, M. L. 1989 *Phys. Rev.* A **40**, 1515.

Shan, X. & Montgomery, D. 1993*a* *Plasma Phys. Contr. Fusion* **35**, 619.

Shan, X. & Montgomery, D. 1993*b* *Plasma Phys. Contr. Fusion* **35**, 1019.

Shan, X., Montgomery, D. & Chen, H. 1991 *Phys. Rev.* A **44**, 6800.

Taylor, R. J., Brown, M. L., Fried, B. D., Grote, H., Liberati, J. R., Morales, G. J. & Pribyl, P. 1989 *Phys. Rev. Lett.* **63**, 2365.

Tynan, G. R., Schmitz, L., Conn, R. W., Doerner, R. & Lehmer, R. 1992 *Phys. Rev. Lett.* **68**, 3032.

Zohm, H., ASDEX-Upgrade Team, and NI and ICRH Group 1994 *Phys. Rev. Lett.* **72**, 222.